JOURNAL OF APPLIED ELECTROCHEMISTRY 16 (1986) 147–155

Activity of anodic oxide films on metal and cermet anodes in cryolite–alumina melts

P. G. RUSSELL*

Great Lakes Research Corporation, P.O. Box 1031, Elizabethton, Tennessee 37643, USA

Received 15 January 1985; revised 18 March 1985

The activity of anodic oxide films on nickel, iron and copper metal anodes in cryolite–alumina melts was calculated using values of the reversible potential obtained from a polarization scan of the corresponding metal electrode. The best results were obtained with prepolarized electrodes. The anodic oxide layer formed on nickel becomes thick and dense and remains adherent during the period of prepolarization. Similar activity calculations were made for selected nickel–, iron– and copper–cermet compositions containing either a MnZn ferrite or a nickel ferrite ceramic phase. Large activities were observed for a NiO type corrosion product on both the nickel and nickel–cermet electrodes. The results suggest that a dense surface layer containing a NiO phase is formed on nickel–cermet electrodes. This layer may help lower corrosion by minimizing electrolyte penetration of the anode surface.

1. Introduction

Development of a non-consumable anode for the Hall–Heroult process with an acceptable corrosion rate is made difficult by the aggressive nature of the cryolite electrolyte towards most metals, refractory hard metals and ceramic oxide compositions. In one study by Kronenberg [1], anode potential sweep data showed that a solid copper rod is more stable than a nickel rod, i.e. had a larger anode potential for a given current density. Both metals were observed to be much more stable than a solid 50% TiB_2–50% BN electrode composition. Electrode stability has been observed to increase when anodes are fabricated from selected ceramic oxide compositions, e.g. many SnO_2 compositions have relatively low corrosion rates. It has also been shown that many simple oxides are stabilized by formation of a complex oxide structure such as a spinel that has a corrosion rate lower than either of the simple oxide components. In recent work it has been observed that cermet compositions make better anodes than complex oxide structures since they have better conductivities and lower corrosion rates. Comparison of various nickel–, iron– and copper–cermet compositions to be discussed in this paper shows that the nickel–cermets experience the lowest corrosion rates during anodic polarization in cryolite–alumina melts. The purpose of this work was to examine the stability of oxide films on pure nickel, iron and copper metal anodes and selected cermet compositions containing these metals.

In a previous study [2] platinum was observed to behave as a reversible O_2 electrode in cryolite baths saturated with alumina. The reversible potential (RP) for platinum measured relative to an aluminum-pool reference electrode was 2.19 V at 970° C. The corrected value of ~2.206 V included a correction for the thermoelectric potential at the Mo/Al interface of the reference electrode and is close to the theoretical value of 2.213 V calculated for the decomposition potential (DP) of alumina at 970° C [3]. In this work values of the RP were observed at nickel, iron and copper metal anodes and cermet anodes of these metals containing either a MnZn ferrite or nickel ferrite spinel ceramic phase. The

* *Present address*: Yardney Corporation, Yardney Battery Division, 82 Mechanic Street, Pawcatuck, Connecticut 06379, USA.

0021–891X/86 $03.00 + .12

difference between the observed values of RP for platinum and a metal anode, i.e. an observed DP, is close to the value of DP calculated for a bath saturated with oxide of the corresponding metal in its lower valence state. Thus, the observed DP can be used to estimate the activity of this oxide film on the corresponding metal anode. In a similar manner oxide activity calculations were made for selected nickel–, iron– and copper–cermet compositions.

2. Experimental details

A description of the cell with outer Inconel jacket for atmosphere control and instrumentation for carrying out electrochemical measurements was described in the previous work [2]. The cryolite–alumina melts contained a nominal 7 wt % CaF_2 and were saturated with both alumina and aluminium metal. The cryolite ratio (on a weight basis) varied from ~1.0 to 1.15.

The metal anodes were made from high-purity rods 6 mm in diameter and 25 mm in length. In order to avoid a thermoelectric potential, high-purity 2 mm diameter wire of the corresponding metal was heli-arc welded to each anode. High-purity metal and ceramic oxide powders were used in the fabrication of cermet anode compositions. Standard ceramic processing methods gave cermet anodes with a theoretical density of above 98%. An alumina sheath provided anode support and limited the active surface area to the bottom face of each metal or cermet anode.

Electrode prepolarization was carried out with an anodic current of 1 A. For metal anodes this is equivalent to a current density of ~3125 mA cm^{-2}. Most polarization measurements were made by scanning the anode potential at a rate of $+0.2\,mV\,s^{-1}$ relative to an aluminum-pool reference electrode starting at a potential on the cathodic branch of the polarization curve. A few runs were made by reversing this procedure and scanning to lower potentials from a starting point on the anodic branch.

3. Results and discussion

A portion of the cathodic and anodic branches of a typical polarization curve for nickel, iron and copper anodes is shown in Fig. 1. The potential at the intersection of these branches is taken as the observed value of RP. The digital readout of anode potential was recorded for the lowest current observed on an x–y recorder during the polarization scan. The observed values of RP for most nickel and iron polarization curves are easy to obtain since the anodic and cathodic branches meet at a given value of potential. Comparison shows that the potential of intersection for copper is not as well defined, and for the curve shown in Fig. 1 the value of RP is observed over a region of 20 mV. Reversible potential values are listed in Table 1 for nickel, iron and copper anodes. Comparison of the results for nickel shows that the largest values of RP (scans 2–4) were observed when an 'adequate' amount of oxide was formed on the anode during prepolarization. In the absence of or with a limited period of prepolarization, e.g. 5 min, the values of RP covered a wide range

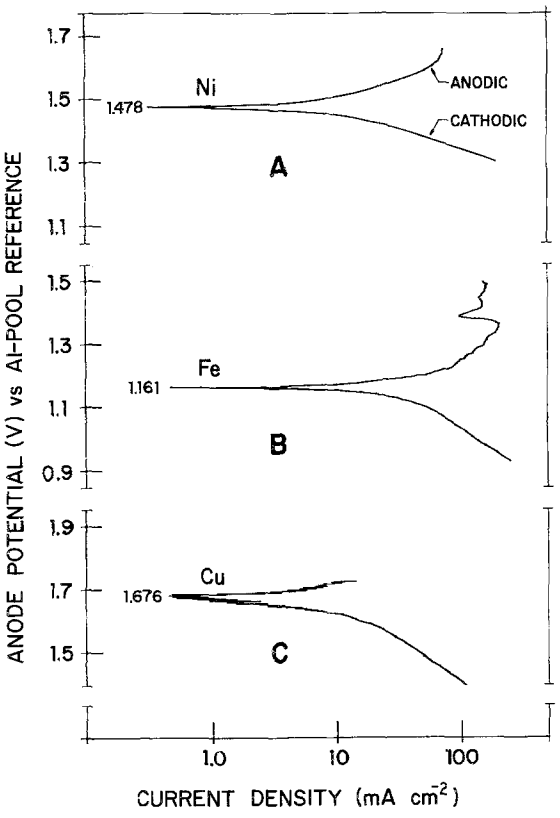

Fig. 1. Polarization curves for nickel, iron and copper anodes. Curves are shown for runs 3(A), 8(B) and 11(C) in Table 1.

Table 1. Reversible potential of nickel, iron and copper anodes in cryolite–alumina melts

Run number	*Prepolarization time (min)*	*Final anode* potential (V)*	*Bath temperature (°C)*	*Reversible potentials (V)*	*Sparging gas*
Nickel anode					
1	0		971	1.381	Ar
2	12	7.74	974	1.468	O_2
3	7†	7.90	965	1.478	Ar
4	8†	8.70	971	1.484	O_2
5	15	8.48	970	1.440	Ar
Iron anode					
6	8	3.12	971	1.077	Ar
7	20†	3.37	970	1.133	Ar
8	25	3.52	971	1.161	Ar
9	25	3.12	970	1.111	O_2
Copper anode					
10	10	2.77	970	1.670	O_2
11	10	2.74	970	1.676	O_2
12	0		964	1.650‡	Ar
13	10†	2.76	970	1.672	Ar

* Potential at end of prepolarization period.
† Additional period of anodic polarization follows previous run.
‡ Copper anode kept cathodic at + 1.161 V for 30 min during bath sparging with argon prior to this scan.

(1.185–1.425 V). Similarly, the largest value of RP for iron and copper anodes was observed during scans following a period of prepolarization. The RP values appear to be independent of dissolved O_2 since the results are similar for both sparging with either O_2 or argon. This insensitivity may be due in part to the limited solubility of O_2 in cryolite–alumina melts [4] and suggests that the cathodic current is due primarily to metal oxide reduction. The RP value for nickel in particular is close to the theoretical value expected for a nickel electrode in a cryolite melt saturated with NiO, i.e. when the activity of dissolved oxide is 1. In this case the cathodic current is provided by reduction of surface oxide and/or dissolved nickel species near the anode surface. A high activity for dissolved nickel species is expected only near the anode surface and this may limit its contribution to the cathodic current during a slow polarization scan.

The rapid increase in potential at a nickel anode during prepolarization suggests that the initial oxide layer forms a thick film with a passive oxide structure which remains adherent to the electrode surface. Typical prepolarization curves for nickel, iron and copper anodes are shown in Fig. 2. The increase in potential observed initially for iron and copper anodes is followed by a period of slow but steady growth suggesting that a near steady-state condition is reached after a few minutes between the formation and dissolution of anodic oxide on the electrode surface. By comparison, the potential for nickel, which shows a slow growth rate during the initial period of oxide formation, starts to increase rapidly at some time in the interval 3–10 min depending on polarization history, i.e. on the amount of prepolarization received by the nickel anode during one or more previous scan experiments. For example, after a total of 19 min of prepolarization in runs 2 and 3 of Table 1 the potential increased rapidly after 2 min of the third prepolarization period in run 4. These qualitative results for nickel suggest that a porous layer is formed during the intial period of oxide formation during which time the anode potential increases at a slow rate. Conversion to a thick, dense passive layer which remains adherent to the electrode surface would

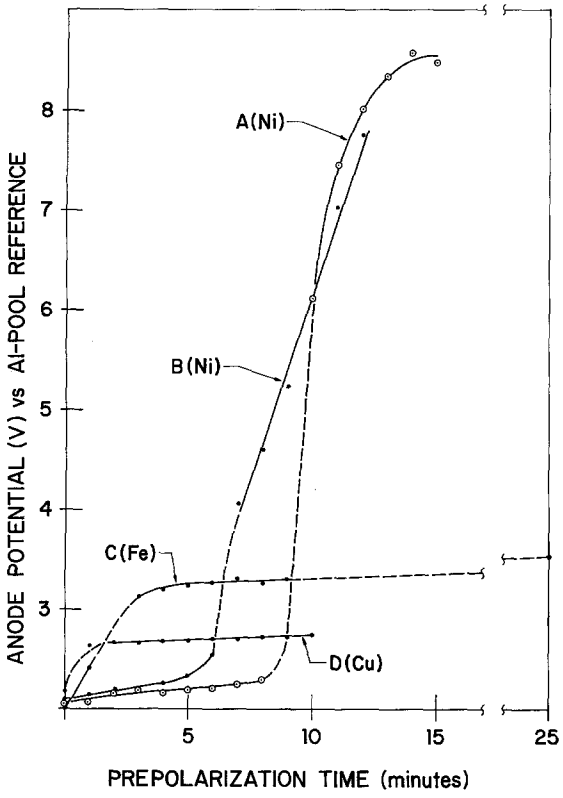

Fig. 2. Prepolarization curves for nickel, iron and copper anodes. Curves are shown for runs 5(A), 2(B), 8(C) and 11(D) in Table 1. ---, estimated path.

account for the rapid increase observed in anode potential as shown in Fig. 2. Barrier attack by the electrolyte is observed here. Above 7 V the anode potential fluctuates erratically by ± 1 V from the estimated average values plotted in Fig. 2, most likely because of breakdown in the dielectric or insulating properties of the oxide structure. As a result, further nickel corrosion is required to keep the oxide barrier in a state of repair. In contrast, only small variations were observed in the anode potential of iron and especially copper during prepolarization measurements.

The activities listed in Table 2 were obtained from calculated and observed DP values for the most likely surface oxide candidates. The values of observed DP were obtained from

$$\text{DP(observed)} = 2.19 - \text{RP}$$

where 2.19 is the potential of the reversible O_2 electrode measured relative to an aluminum-pool reference and RP is the largest value of the reversible metal electrode potential from Table 1. Metal oxide activity (a_{oxide}) is given by the following equation:

$$\text{DP(observed)} = \text{DP(calculated)} - \frac{2.303RT}{nF} \log a_{\text{oxide}}$$

where n is 2 except for Fe_2O_3 where n is 6.

Table 2. Activity of oxide films on metal anodes

Run number in Table 1	*Metal oxide*	*Calculated* DP (V)*	*Observed DP (V)*	*Oxide activity*
4	NiO	0.693†	0.706	0.78
		0.663‡	0.706	0.45
8	FeO	0.993	1.029	0.51
	Fe_2O_3	0.867	1.029	1.1×10^{-4}
11	Cu_2O	0.415	0.514	0.16
	CuO	0.243	0.514	6.3×10^{-3}

* Free energy for metal oxide formation taken from JANAF Thermochemical Tables [3], except where noted.
† Reference [5].
‡ Reference [6].

The largest activities were obtained for NiO, FeO and Cu_2O which indicates that these oxides are the stable component of the oxide layer on the respective metal anode during potential scan measurements. Formation of oxide structures containing these lower valence state cations may occur during prepolarization. However, conversion of higher oxide components formed during anodic polarization to the above oxide structures during a slow potential scan along the cathodic branch could give the same results. The oxide activity on nickel was calculated for ΔG values obtained from two sources [5, 6]. The largest oxide activity on nickel calculated as NiO is 0.78. The smaller value, 0.45, is similar to the value of 0.51 observed for FeO on iron. The smallest value, 0.16, was obtained for Cu_2O on copper. The relatively large oxide activity on nickel is further evidence that a thick, nonporous and adherent layer is formed during prepolarization.

Chemical and electrochemical attack at the metal/melt interface cause metal anodes such as nickel, iron and copper to corrode rapidly in cryolite–alumina melts. The rate of attack is influenced by the stability of surface oxide

Table 3. Oxide solubility and ratio of activities of metal fluoride to metal oxide in a cryolite melt saturated with alumina at 970° C

Oxide	*Solubility (wt %) in 95 wt % cryolite + 5 wt % alumina*	a_{MF_2}/a_{MO}*
NiO	0.18	1.0×10^{-3}
FeO	6.0	2.1×10^{-3}
Fe_2O_3	0.003	8.0×10^{-5}†
Cu_2O	–	4.5×10^{-6}‡
CuO	0.68	6.4×10^{-5}

* Activities were calculated with ΔG_f^0 values obtained at 970° C from the following equation, [8]: $3/y(M_xO_y) + 2AlF_3 = 3x/y(MF_{2y/x}) + Al_2O_3$, where $a_{Al_2O_3}$ is 1 for a saturated bath and $-\log a_{AlF_3}$ is 2.737 for an Al_2O_3-saturated melt with bath ratio of 1.1 at 1005° C, [9]. The ΔG values for all oxides and fluorides were taken from [3] with the following exceptions: ΔG for NiO, [6] and an estimation of ΔG for NiF_2, [10].
† $a_{FeF_3}/a^{1/2}Fe_2O_3$.
‡ $a_{CuF}/a^{1/2}Cu_2O$.

formed during the corrosion process. While an adherent film would tend to impede anode attack, a highly soluble and/or conversion of this oxide to a soluble fluoride would enhance the corrosion process. Solubilities and ratios of activities of metal fluoride to metal oxide are given in Table 3. Both FeO and CuO are more soluble than NiO in molten cryolite containing 5 wt % Al_2O_3 [7]. Their greater solubility may limit oxide growth and thereby account for the near steady state behaviour for iron and copper anodes soon after the start of prepolarization whereas the lower solubility of NiO would enhance the growth of surface oxide. Conversion of surface oxide to a soluble fluoride does not appear to be an important factor since the ratios in Table 3 are 10^{-3} or smaller.

Anode corrosion rates can be reduced substantially by using some ceramic oxides and especially cermet electrode compositions. A number of ceramic oxide compositions corrode at a slower rate than most metals in cryolite–alumina melts. Complex oxides, being less soluble, corrode less than simple oxides. The solubility of a simple oxide in a cryolite–alumina melt decreases when the oxide is stabilized in a complex oxide structure, e.g. the solubility of a $NiFe_2O_4$ spinel is lower than the solubility of either the NiO or Fe_2O_3 oxide components [8, 11]. The corrosion rate of an anode made from a complex oxide such as a ferrite spinel may also be reduced further in cermet form. Anode corrosion rates were obtained for a number of nickel–, iron– and copper–cermet compositions. These screening experiments were carried out for a period of 24 h under electrolysis conditions in a large test cell constructed for this purpose. See [12] for a detailed description of this test cell, measurement of bath parameters and electrolysis conditions used for measuring anode corrosion rates during 100-h corrosion tests. The corrosion test results show that Ni/(Mn, Zn) ferrite and Ni/Ni ferrite Ni–cermet compositions corrode at a much slower rate than either the nickel metal or ferrite components, e.g. cermets, 50–100 mm per year; $NiFe_2O_4$, 200 mm per year. A further comparison shows that iron and copper-based cermet electrodes with the above ferrite spinel structures corrode at a much faster rate than the corresponding nickel–cermet compositions.

Stabilization of a simple oxide in a spinel structure should affect its activity, and hence a change in the value of RP is expected for the above cermet compositions, e.g. for an increase in activity the RP would be larger. In addition, a mixed potential is possible when more than one cation is present in the spinel structure. This would also cause a change in RP. The values of RP for a number of nickel–, iron– and copper–cermets containing a (Mn, Zn)$Fe_{2.04}O_4$ ceramic phase are listed in Table 4. Polarization curves for the nickel–cermets in runs 1, 2 and 5 are shown in Fig. 3. The values of RP for many of the nickel–cermet anodes agree well with values observed for the nickel anodes in Table 1. The values listed here range from 1.47 to 1.502 V for the Mn, Zn ferrite compositions with the exception of run 5. (In this case extensive prepolarization and scanning to lower potentials shifted the RP value to 1.64 as shown in Fig. 3c.) In the absence of prepolarization, a small amount of adherent anodic oxide is formed at the surface of the nickel metal phase during pen alignment prior to recording of the polarization scan. An increase in current density expected in the metal component of the ceramic surface because of the high metal conductivity would enhance the

Table 4. Reversible potential of nickel–, iron– and copper–cermet anodes containing a $(Mn,Zn)Fe_{2.04}O_4$ ceramic phase

Run number	*Metal phase (vol%)*	*Prepolarization time (min)*	*Final anode* potential (V)*	*Bath temperature (°C)*	*Reversible potential (V)*	*Sparging gas*
1	7 Ni	0	–	970	1.488 1.545†	O_2
2	16 Ni	0	–	971	1.476 1.550‡	O_2
3		0	–	971	1.502 1.535‡	O_2
4	25 Ni	0	–	973	1.502 1.550‡	O_2
5		30	~4.30	969	1.540§ 1.640‖	O_2
6	40 Ni	0	–	~970	1.470	none
7	16 Fe	30	–	969	1.760	O_2
8		10	2.94	971	1.644	Ar
9		10¶	2.93	970	1.638	Ar
10		33¶	3.00	970	1.672	O_2
11	16 Cu	20	3.08	971	2.135‖	O_2
12		20	2.95	971	1.655	O_2

* Potential at end of prepolarization period.
† Sharp decrease in anodic current density (see Fig. 3A).
‡ Small dip in anodic current density (see polarization curve for run 2 in Fig. 3B).
§ Small break in cathodic current density (see Fig. 3C).
‖ Start at anodic potential for current of 1A and scan to lower voltage.
¶ Additional period of anodic polarization following previous run.

formation of an adherent NiO layer. In this case the Ni/NiO couple is expected to determine the potential–current profile and therefore the RP value. Values for the RP obtained from polarization scans run on two 16 vol % Ni/Ni ferrite cermet samples with the same composition are listed in Table 5. Polarization curves for these samples are shown in Fig. 4. The value of 1.505 V observed with the first sample in run 1 is in good agreement with the RP values for runs 3 and 4 of Table 4. Different results were obtained with the second sample in runs 2 and 3, however. In each case only a small dip was observed in the cathodic current at ~1.44 V which is near the RP expected for the Ni/NiO couple. Small changes in microstructure most likely account for the difference observed here*.

* Microstructure is affected by changes in the sintering cycle. Sample 1 was sintered for 2 h at 1225° C in a vacuum. Sample 2 was sintered for 30 h at 1325° C in a N_2 atmosphere. Surface nickel was apparently converted to an oxide structure by the water vapour and/or O_2 present in the N_2 during the long sintering cycle. As a result of this decrease in nickel activity the RP expected for nickel at ~1.5 V was not observed with this sample.

In runs 1 to 4 of Table 4 and run 1 of Table 5 a passivating layer formed during the initial oxidation of nickel caused either a sharp decrease or a small dip in the anodic current density at a potential of ~1.55 V. However, the current decrease observed in run 1 for Table 4 (Fig. 3A) was not reproducible during one attempt where the active electrode surface was not repolished to remove previously formed anodic oxide. In run 2 of Table 5 (Fig. 4B) the sharp decreases in current density associated with passivation were observed in the interval 1.514 to 1.55 V. An EDX analysis has shown that a small amount of iron is present in the nickel phase. Iron may affect the electronic properties such that the initial anodic oxide layer acts as an insulator since there is no evidence for a similar passivation occurring with a pure nickel rod (Fig. 1A).

Activity values calculated for oxide films on nickel–, iron– and copper–cermet anodes are listed in Table 6. For a NiO DP of 0.693 V, the oxide activity increases from a value of 0.78 for a nickel anode to a value of ~1 for both

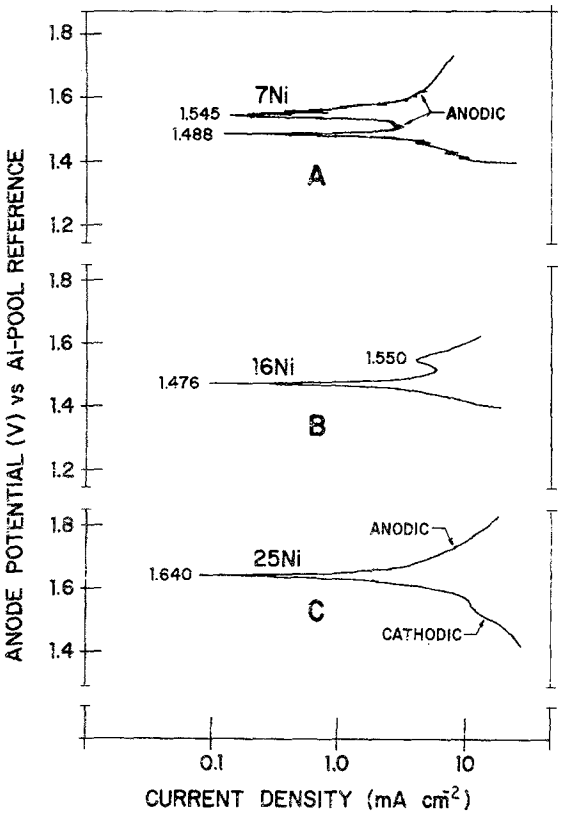

Fig. 3. Polarization curves for selected Ni/(Mn,Zn)$Fe_{2.04}O_4$ cermet anodes. Curves are shown for runs 1(A), 2(B) and 5(C) in Table 4. Metal phase given in vol %.

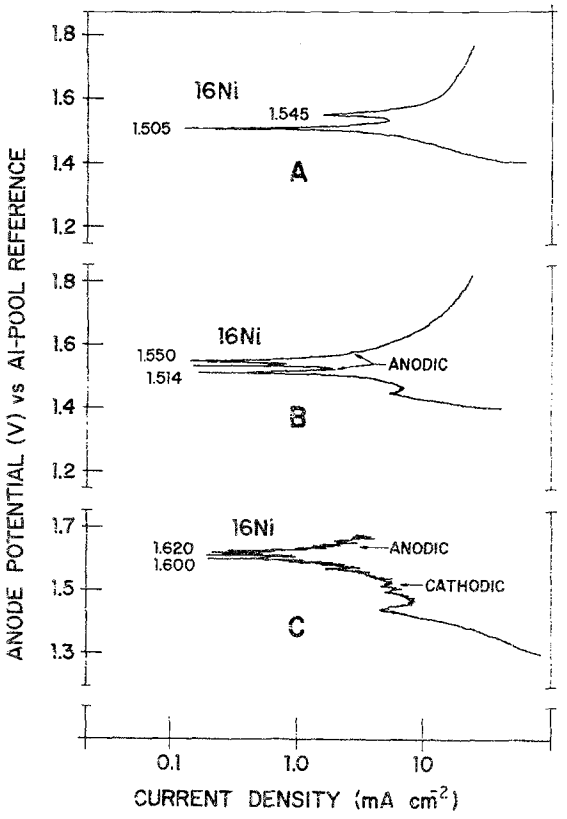

Fig. 4. Polarization curves for two 16 vol % Ni/$NiFe_{2.04}O_4$ anodes. Curves are shown for runs 1(A), 2(B) and 3(C) in Table 5. Metal phase given in vol %. First sample, run 1; second sample, runs 2 and 3.

nickel–cermet compositions. A large oxide activity indicates that the surface oxide formed during anodic polarization, i.e. NiO is present as a dense adherent layer on the 'nickel phase' of the active surface. Reaction of a part of this oxide with the adjacent ferrite spinel component to form a stabilized surface oxide layer that remains dense and adherent would minimize electrolyte penetration of the anode surface and help explain the low corrosion rates observed with nickel–cermet compositions. Stabilization energy for this solid-state interaction can be as high as 12 kcal mol^{-1} for spinel oxide structures [8] and may involve the diffusion of cations in spinel and NiO-type structures [13]. In a previous work [13] the examination of nickel–cermets containing a $NiFe_2O_4$ spinel phase has shown that the cermet material becomes oxidized during Hall-cell electrolysis and that the oxidized product close to the cermet/cryolite interface forms a relatively dense layer. Microprobe analysis was used to identify spinel-like phases and an iron oxide phase as the components of this layer. In the present work, measurement of oxide activity by an *in situ* method suggests that a NiO phase could be one component involved in the formation of a dense surface oxide structure.

The RP values observed for the iron–cermet compositions in Tables 4 and 5 are larger than the values observed for the iron rod anode listed in Table 1. The value of 1.284 V in run 6 of Table 5 suggests that Fe_2O_3 with an activity of ~ 0.11 is the dominant oxide on the 'iron metal' phase of the active surface of the 16 vol % Fe/$NiFe_{2.04}O_4$ cermet composition after extensive prepolarization. This low value indicates a lack of surface oxide stabilization which may account for the large corrosion rates observed with iron–cermet compositions. The larger RP values observed for the 16 vol % Fe/(Mn,Zn)

Table 5. Reversible potential of nickel–, iron– and copper–cermet anodes containing a $NiFe_{2.04}O_4$ ceramic phase

Run number	*Metal phase (vol%)*	*Prepolarization time (min)*	*Final anode* potential (V)*	*Bath temperature (°C)*	*Reversible potential (V)*	*Sparging gas*
1	16 Ni	0	–	~973	1.505 1.545†	O_2
2		0	–	969	1.445‡ 1.514–1.55§	O_2
3‖		0	–	971	~1.440¶ 1.60–1.62	O_2
4	16 Fe	12	3.08	970	1.244	O_2
5		12**	3.14	972	1.268	O_2
6		30**	–	972	1.284	O_2
7	16 Cu	10	3.26	970	1.456	O_2
8		10**	3.30	968	1.624	Ar
9		40**	3.19	968	1.703	Ar

* Potential at end of prepolarization period.
† Sharp decrease in anodic current density (see Fig. 4A).
‡ Small dip in cathodic current density (see Fig. 4B).
§ Three or more sharp decreases in current density were observed in this interval of anode potential (see Fig. 4B).
‖ This run was made at a later date with sample from run 2 without polishing surface to remove oxide product of previous polarization scan.
¶ Small break in cathodic current density (see Fig. 4C).
** Additional period of anodic polarization following previous scan.

$Fe_{2.04}O_4$ cermet compositions in Table 4 are most likely the result of a mixed potential involving manganese and/or zinc oxide activity.

Similar RP values were observed for both copper–cermet compositions. The increase to a value of 2.135 for run 11 in Table 4 results from scanning to lower potentials. For the largest value observed in Table 5 (run 9), the oxide activity calculated as Cu_2O is ~0.26 which is an increase of 0.1 over the value in Table 2. Again, this low value suggests a lack of surface oxide stabilization and as in the case of iron–cermets it may serve as an indicator for the large corrosion rates observed with copper–cermet compositions.

Table 6. Activity of oxide films on cermet anodes

Run number	*Metal oxide*	*Calculated* DP (V)*	*Observed DP (V)*	*Oxide activity*
3 (Table 4)	NiO	0.693†	0.688	1.00
		0.633‡	0.688	0.63
6 (Table 5)	Fe_2O_3	0.866	0.906	0.11
9 (Table 5)	Cu_2O	0.416	0.487	0.26

* Free energy for metal oxide formation taken from JANAF Thermochemical Tables [3] except where noted.
† Reference [5].
‡ Reference [6].

4. Conclusion

1. Reversible potential measurements provide an *in situ* method for obtaining the activity of surface oxide formed during anodic polarization in a cryolite–alumina electrolyte.

2. The activity of ~0.78 calculated for NiO on nickel suggests that a dense adherent layer of this oxide is formed on a nickel electrode. The lower values calculated for the activities of oxides on iron and copper suggest that these surface layers are less stable, most likely because of the increased oxide solubilities in cryolite–alumina melts.

3. The activity of surface oxide calculated for NiO is close to one for nickel–cermets, suggesting that a NiO phase may play a major role in the formation of a dense, adherent surface oxide layer which helps minimize electrolyte penetration of the anode surface.

Acknowledgements

The author would like to thank T. E. Landon

for preparation of the cermet electrodes and G. Holly for final electrode assembly and bath maintenance. He is also indebted to Dr J. M. Clark and Dr D. R. Secrist (supervisor) for a critical reading of this manuscript. Several of their suggestions have been included in the final version. The author is grateful to GLRC for financial support of this project.

References

[1] M. L. Kronenberg, *J. Electrochem. Soc.* **116** (1969) 1160.

[2] P. G. Russell, in 'Fourth International Symposium on Molten Salts' (edited by M. Blander, D. S. Newman, M-L. Saboungi, G. Mamantov and K. Johnson), The Electrochemical Society, Pennington, NJ (1983) p. 430.

[3] JANAF Thermochemical Tables, 2nd edn, Dow Chemical Company, Midland, Michigan (1971).

[4] 'Inert Anodes for Aluminium Smelting', Eighth Interim Technical Report for the period 1982 July 01–1982 September 30, Aluminum Company of America, Alcoa Laboratories, Alcoa Center, Pennsylvania (January 1983) p. 9.

[5] A. Glossner, US Atomic Energy Commission Report, ANL 5750.

[6] S. Bergland, *Ber. Bunsenges. Phys. Chem.* **80** (1976) 862.

[7] K. Grjotheim, C. Krohn, M. Malinovsky, K. Matiasovsky and J. Thonstad, 'Aluminum Electrolysis. The Chemistry of the Hall–Heroult Process'. Aluminum-Verlag, Dusseldorf (1977).

[8] K. Horinouchi, N. Tachikawa and K. Yamada, Proceedings of First International Symposium on Molten Salts in Chemistry Technology, Kyoto, Japan, 20–22 April, 1983. Paper B-209.

[9] A. Sterten and K. Hamberg, *Light Met., Proc. Sess., AIME Annu. Meet.* **1** (1976) 203.

[10] G. Chattopadhyay, M. D. Karkanavala and M. S. Chandrasekharaiah, *J. Electrochem. Soc.* **122** (1975) 325.

[11] 'Inert Anodes for Aluminum Smelting', Ninth Interim Technical Report for the period 1982 October 01–1982 December 31, Aluminum Company of America, Alcoa Laboratories, Alcoa Center, Pennsylvania (May 1983) p. 4.

[12] J. M. Clark, 'Anodic Corrosion of Sintered Oxide Materials in Hall–Heroult Melts'. Extended Abstracts No. 435, Fall Meeting of the Electrochemical Society, Washington, DC, October 9–14, 1983.

[13] 'Inert Anodes for Aluminum Smelting', Final Technical Report for the Period 1980 October 01–1981 September 30, Aluminum Company of America, Alcoa Laboratories, Alcoa Center, Pennsylvania (January 1983) p. 11.